Evolution of superconductor pairing interactions from weak to strong coupling on a honeycomb lattice

Shi-Quan Su,[1,2] Ka-Ming Tam,[3] and Hai-Qing Lin[1]

[1]*Department of Physics and Institute of Theoretical Physics, The Chinese University of Hong Kong, Hong Kong, China*
[2]*Department of Physics and Astronomy, Louisiana State University, Baton Rouge, Louisiana 70803, USA*
[3]*Department of Physics and Astronomy, University of Waterloo, Waterloo, Ontario, Canada N2L-3G1*

We study the evolution of the pairing from weak to strong coupling on a honeycomb lattice by quantum Monte Carlo. We show numerical evidence of the BCS-Bose-Einstein condensation (BEC) crossover as the coupling strength increases on a honeycomb lattice with small Fermi surface by measuring a wide range of observables: double occupancy, spin susceptibility, local pair correlation, and kinetic energy. Although at low energy, the model sustains Dirac fermions, we do not find significant qualitative difference in the BCS-BEC crossover as compared to those with an extended Fermi surface, except at weak-coupling, BCS regime.

I. INTRODUCTION

It has long been known that the pairing formed from an attractive coupling has a smooth crossover between the weak coupling and the strong coupling.[1–3] In the weak-coupling limit, singlet pairs are formed around the Fermi surface, according to the BCS theory. In the strong-coupling limit, local bound pairs can be formed, and these "preformed pairs" condense as the temperature is further lowered where the Bose-Einstein condensation (BEC) occurs. The interest on this crossover has been revitalized[4–10] mainly due to the quest of understanding the pseudogap phase in the high-temperature superconductors.

Recently, condensed-matter systems sustain on fermions with linear dispersion, typical examples are honeycomb lattice models and nodal fermions for d-wave superconductors, have generated huge surge of intensive studies. These models possess substantial differences from models with extended Fermi surface such as models on square lattice. In particular, it has been suggested that the quantum phase transition (QPT) between the metallic phase and the degenerate charge-density wave/pairing phase at half filling in the attractive Hubbard model (AHM) on honeycomb lattice is related to its BCS-BEC crossover away from half filling.[11] This certainly does not happen on the square lattice, in which the flat Fermi surface at half-filling renders the Umklapp scattering becoming the dominant channel, its BCS-BEC crossover is not related to any QPT through tuning the attractive coupling.[12] In the honeycomb lattice, the density of state is zero at half filling, therefore any instability from the band structure is weakened and strong coupling is needed to induce ordering. It can be shown that all the short-range interactions are irrelevant. In order to tackle the strong-coupling problem, besides breaking the symmetry by mean-field ansatz, we choose quantum Monte Carlo (QMC) method in this work to study the BCS-BEC crossover in the honeycomb lattice.

Various studies[6,13–15] have been devoted to the BCS-BEC crossover of the AHM on a square lattice. The objective of this work is to study how do the linear dispersion and the aforementioned QPT at half filling affect the BCS-BEC crossover of the slightly doped system.

Our main finding can be summarized as follow. At the weak-coupling, BCS-like regime, pseudogap phenomena are observed, however we expect that it is mainly due to the band structure of honeycomb lattice, rather than the bound pair formation. At the intermediate coupling, crossover regime, we can identify two temperature scales, the high temperature one where the performed pair formed with associated pseudogap phenomena; and the low temperature one where the system enters the pairing phase. At strong-coupling, BEC-like regime, the electrons form pairs at high temperature and condense as hardcore bosons at low temperature. However, we do not find distinctive feature compares to the square lattice, except at the weak-coupling regime where the band structure dominates the quasiparticle dispersion.

II. MODEL AND METHOD

The AHM in honeycomb lattice reads

$$H = -t \sum_{\langle i,j \rangle, \sigma} c_{i\sigma}^{+} c_{j\sigma} - U \sum_{i} n_{i\uparrow} n_{i\downarrow} - \mu \sum_{i\sigma} n_{i\sigma}, \quad (1)$$

where $c_{i\sigma}(c_{i\sigma}^{+})$ annihilates (creates) a particle with spin σ at site i, $\langle i,j \rangle$ denotes the nearest-neighbor lattice sites i and j, t is the hopping matrix element, U is the on-site attractive interaction, and μ is the chemical potential. In the following we set $t=1$ as the energy scale of the system. The bare electronic ($U=0$ limit) dispersion is given by $\epsilon_{\mathbf{k}} = \pm \sqrt{3 + 2\cos(\sqrt{3}k_y) + 4\cos(\sqrt{3}k_y/2)\cos(3k_x/2)}$ and the band width W is 6. At half filling this is linear around the Fermi points. Keeping only the low energy excitations, in the first quantized form the wave function follows the two-dimensional Weyl equation for massless chiral Dirac fermions, $v_F\hat{\sigma}\cdot\nabla\Psi(\mathbf{r})=E\Psi(\mathbf{r})$, where $\hat{\sigma}=(\sigma_x,\sigma_y)$ are the Pauli matrices and $v_F=3/2$ is the Fermi velocity. This description in term of Dirac fermions is not exact away from half filling. Nevertheless, the linear dispersion can be a good approximation below the van Hove singularities at filling $n=1\pm1/4$. For this reason, we choose $n=0.88$ for our calculations using determinant quantum Monte Carlo (DQMC).[16]
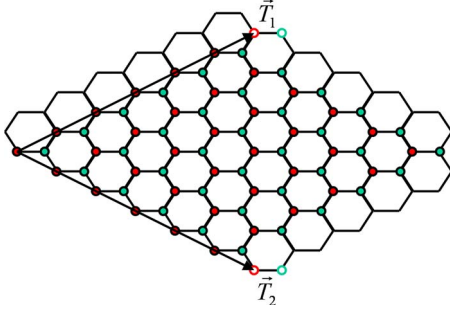
FIG. 1. (Color online) Sketch of a 72 sites honeycomb lattice. The solid circles are the lattice points in the honeycomb lattice. The two triangular sublattices are labeled by different colors. $\vec{T}_1$ and $\vec{T}_2$ are the real-space translational vectors.

The DQMC (Refs. 16 and 17) is a Hamiltonian based approach. The Hamiltonian H in the partition function $Z = \text{Tr} \exp(-\beta H)$ is expressed in the real space via the Trotter decomposition and Hubbard-Stratonovich (HS) transformation. The only systematic error is from discretizing the imaginary time β into M slices of $\Delta\tau = \beta/M$ in the Trotter decomposition. The HS transformation replaces the on-site interactions in the attractive Hubbard model by HS fields coupled to the charge. The summation over the HS fields is treated by Monte Carlo procedure. The calculations are proceeded on a $N=72$ sites honeycomb lattice, the actual lattice for the simulation is shown in the Fig. 1. Since the attractive Hubbard coupling does not have minus-sign problem, a wide range of temperatures and couplings can be studied.

III. QMC RESULTS

One of the clear signals indicating the formation of bound pairs at strong coupling is the formation of spin gap. At weak coupling, we expect fermion quasiparticle character to remain at high temperature, for which the spin susceptibility increases as the temperature is lowered. On the other hand, the strong-coupling limit is manifested by the decrease in the spin susceptibility as the temperature is lowered, due to the formation of the gap which leads to the reduction in the spectral function at low frequency.

We first show the spin susceptibility $\chi(\mathbf{q}, \omega)$ at frequency $\omega = 0$ and momentum $\mathbf{q} = (0,0)$ in Fig. 2, where we also show the spin susceptibility from random-phase approximation (RPA) calculation for comparison. $\chi(0,0)$ is suppressed for all couplings, as can be inferred simply from the RPA formulation, where $\chi_{\text{RPA}}(0,0) = \chi_0(0,0)/[1 + U\chi_0(0,0)]$. At weak coupling $\chi(0,0)$ increases as the temperature is lowered as expected for a fermion quasiparticle description, however it bends downward before it goes upward again as the temperature is lowered further. This two peak structure of $\chi(0,0)$ associated with the formation of the pseudogap has been found in the dynamical mean-field-theory study.[6] However, in the honeycomb lattice, the apparent pseudogap phenomena indicated by this structure of $\chi(0,0)$ already exist in the weak-coupling regime, below the strong-coupling regime where the "preformed pair" phenomena occur. Therefore, we believe that it is derived from the particular dispersion rela-
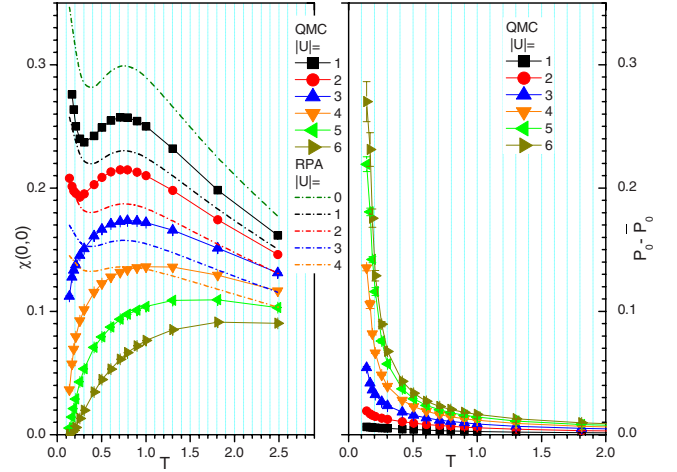

FIG. 2. (Color online) Uniform spin susceptibility $\chi(0,0)$ (left) and pairing correlation function $P_0 - \bar{P}_0$ (right) as a function of temperature for a range of interaction strength at $n=0.88$.

tion of honeycomb lattice, where the density of state is small around the doped Fermi surface.

On the other hand, in the strong-coupling regime, $\chi(0,0)$ vanishes quickly as the bound pairs are formed and spin gap equals the binding energy needed to break the pair. In the weak-coupling regime, the QMC results behave similarly as compared to the RPA results. When the interaction is increased to around $W/2$, the QMC results evolve in the opposite direction as compared to the RPA results and drop sharply at low temperature, whereas the RPA results at low-temperature limit do not change qualitatively when U increases. This signals that the system enters the phase in which electrons form bound pairs and the spin excitations start to be gapped.[13] The pairing phase cannot be reached by summing the ladder diagrams within the RPA. For strong coupling ($U \approx W$), the suppression of $\chi(0,0)$ becomes smooth and appears at high temperature. This effect reflects the fact that the bound pairs are already formed at high temperature.[14] The temperature where deviations appear between the QMC results and the RPA results is an indication of the formation of local singlet pair, which can be interpreted as the energy scale where the fermion quasiparticle description is not valid for any lower temperature.

We then probe the pairing directly by considering the pairing correlation function for local pairing, $P_0 = \frac{1}{N^2}\Sigma_{l,i}\langle c^{\dagger}_{i+l,\uparrow}c^{\dagger}_{i+l,\downarrow}c_{i,\downarrow}c_{i,\uparrow} + \text{H.c.}\rangle$. The only instability is pairing, in this incommensurate doped case (rules out charge-density wave order). We expect P_0 to increase as temperature is lowered for all coupling strengths. One of the most representative characteristics of local pairs is that they are distributed uniformly in space and condense around zero momentum as bosons when temperature is lowered. This is manifested by the rapid increase in local pair correlation as shown in Fig. 2, note that the single-particle contribution $\bar{P}_0$ has been subtracted from P_0 to emphasize the vertex contribution of pairing.[18] The condensation of the bosonic local pairs for the strong-coupling case ($U=5,6$) can be observed from the rapid increase in $P_0 - \bar{P}_0$ with the decrease in temperature. In contrast, the pairs formed around the quasiparti-
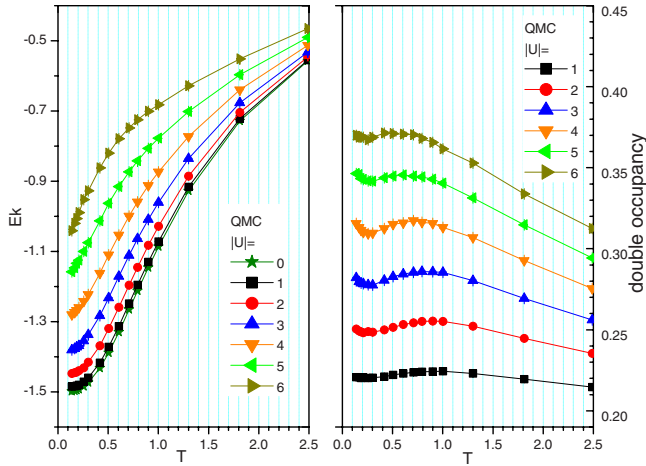
FIG. 3. (Color online) The kinetic energy E_k (left) and double occupancy $\langle n_\uparrow n_\downarrow \rangle$ (right) as a function of temperature for a range of interaction strength at $n = 0.88$.

cle Fermi surface in the weak-coupling regime only bring a slight increase in $P_0 - \bar{P}_0$.

We show the kinetic energy, $E_k = (-t/N) \Sigma_{\langle i,j \rangle, \sigma} \langle c_{i,\sigma}^+ c_{j,\sigma} \rangle$ in Fig. 3. In the weak-coupling regime, its temperature dependence is similar to the free fermion case. When we increase the interaction to the crossover regime ($U \approx 3-4$), qualitative change already happened in the high temperature, where the gain in the kinetic energy is much slower than the free fermion case. Moving into the strong-coupling regime, fermions begin to form bound pairs at high temperature and only lose little kinetic energy. When temperature further decreases, the local pairs in the system condense and hence E_k drops sharply.[14]

A good indicator to measure the local pair formation in the BEC state is the double occupancy $\langle n_\uparrow n_\downarrow \rangle \equiv (1/N) \Sigma_i \langle n_{i,\uparrow} n_{i,\downarrow} \rangle$, see Fig. 3. We find that $\langle n_\uparrow n_\downarrow \rangle$ increases as the temperatures decrease. However, it reaches a local maximum at certain temperature. This can be understood as the change in the kinetic energy which destabilizes the double occupancy. This behavior of $\langle n_\uparrow n_\downarrow \rangle$ are in accord with the fact that the local maximum coincides with the temperature where the kinetic energy drops most sharply. At very low temperature, the bosonic on-site pairs begin to dominate, $\langle n_\uparrow n_\downarrow \rangle$ increases again and should saturate at $n/2$ for strong couplings.

After elaborating the evidence of BCS-BEC crossover, we put those observables from DQMC together and identify the temperature scales for different U. In Fig. 4, we show the results represented for weak ($U=1$), intermediate ($U=3, 4$), and strong ($U=6$) couplings.

At $U=1$, $\chi(0,0)$ QMC result does not deviate from the RPA result. The local pair correlation does not develop, and $\langle n_\uparrow n_\downarrow \rangle$ is small even at low temperature, which shows that the pairing correlation is weak. The critical temperature, T_c, for the Kosterlitz-Thouless transition into the pairing phase is below the lowest temperatures we studied.

At $U=3$, $\chi(0,0)$ local pair correlations begin to increase at $T_c \approx 0.2$. At almost the same temperature the QMC result begins to deviate from the RPA result. These imply the de-
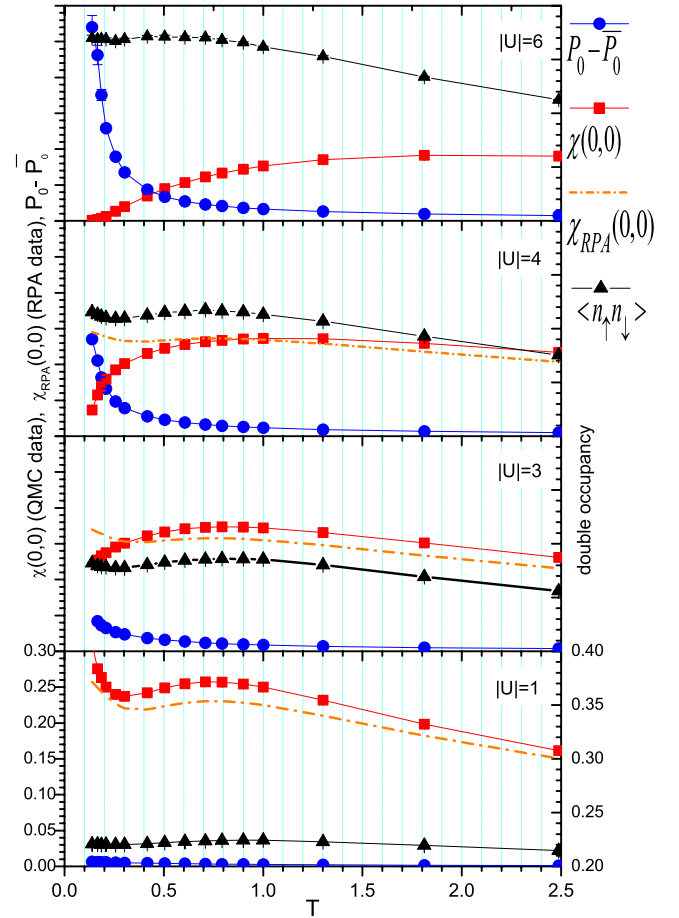

FIG. 4. (Color online) Double occupancy $\langle n_\downarrow n_\downarrow \rangle$, uniform spin susceptibility $\chi(0,0)$ and pairing correlation $P_0 - \bar{P}_0$ as a function of temperature for different coupling strength at $\langle n \rangle = 0.88$ filling.

velopments in both spin and pairing correlations. The system shows BCS-like pairing effect from the instability of the Fermi surface. However, there is no true phase coherence at any finite temperature. Nevertheless, at this coupling strength, the pairing is still rather weak, due to the small density of state around the Fermi energy.

At $U=4$ the system displays two temperature scales. The first one is T^* at high temperature around $T \approx 0.8$, this could be associated with the pseudogap phase. At this temperature, $\chi(0,0)$ from QMC result reaches its maximum and begins to deviate from the RPA result. In addition $\langle n_\uparrow n_\downarrow \rangle$ also reaches the first plateau at high temperature. These signal that electrons bound pairs start to develop, spin gap is formed and the quasiparticle description is broken below this temperature. We estimate the critical temperature for the condensation of bound pairs, $T_c \approx 0.3$. Below this temperature, the local pair correlation $P_0 - \bar{P}_0$ grows quickly and $\chi(0,0)$ drops sharply; $\langle n_\uparrow n_\downarrow \rangle$ reaches its low-temperature maximum and saturates.

At $U=6$, the system is at the strong-coupling limit, where U reaches the band width W, there is only one temperature scale in the system, $T_c \approx 0.5$, within the temperature range we studied. $\chi(0,0)$ reaches its maximum at very high temperature and decreases smoothly, which suggests that pair formation begins at a very high temperature, above the temperature range we studied. Below T_c, $P_0 - \bar{P}_0$ increase

quickly, and $\langle n_\uparrow n_\downarrow \rangle$ tends to $n/2$ at zero temperature. These suggest that the bound pairs undergo a Kosterlitz-Thouless transition, which manifests a BEC-like scenario.

From the above numerically exact DQMC data, we show clearly that there is a qualitative change from weak to strong coupling at finite temperature. This should correspond to the true BCS-BEC crossover at zero temperature. However, we find that the results for the honeycomb lattice have no drastic qualitative difference as compared to that of the square lattice.[14] Certainly, the band structure alters the quantitative values of the coupling for the crossover. However, the BCS-BEC crossover on a doped honeycomb lattice models exists at $U \approx 3-4$ where the linear dispersion approximation for the free fermions is not valid.

IV. DISCUSSIONS AND CONCLUSIONS

With the progress of the techniques of optical lattices and the fabrication of single-layer graphene, the BCS-BEC crossover on a honeycomb lattice and Dirac fermions is not only an important problem itself but also has broad experimental and theoretical interests with other topics under intensive studies.

The atom-atom interaction in ultracold fermionic atoms in an optical trap can be tuned by magnetic field Feshbach resonance. The honeycomb lattice can possibly be realized by optical trap.[19] This may provide a direct way to study experimentally the BCS-BEC crossover problem with linear dispersion.[19] In addition, the superconducting phase of graphene via the attraction from phonons and plasmons has been discussed recently.[20–24] Although it is unlikely to generate strong attraction from phonon coupling in graphene, our results suggest that even at weak-coupling regime, nontrivial temperature dependence of spin susceptibility may occur in the superconducting phase from local Holstein phonon coupling.

In conclusion, we have presented extensive results from DQMC which confirm the BCS-BEC crossover for the doped ($n=0.88$) AHM on a honeycomb lattice. In contrast to the systems with extended Fermi surface, there is an enhancement in pseudogap property revealed from the double-peak structure in the spin susceptibility at weak coupling due to the peculiar density of state of honeycomb lattice. Apart from this, the BCS-BEC crossover does not show prominent difference between square lattice and honeycomb lattice for the parameters and system size we study.

[1] D. M. Eagles, Phys. Rev. **186**, 456 (1969).

[2] A. J. Leggett, *Modern Trends in the Theory of Condensed Matter*, edited by A. Pękalski and J. Przystawa (Springer, Berlin, 1980).

[3] P. Nozières and S. Schmitt-Rink, J. Low Temp. Phys. **59**, 195 (1985).

[4] S. Allen, H. Touchette, S. Moukouri, Y. M. Vilk, and A.-M. S. Tremblay, Phys. Rev. Lett. **83**, 4128 (1999).

[5] B. Kyung, S. Allen, and A.-M. S. Tremblay, Phys. Rev. B **64**, 075116 (2001).

[6] M. Keller, W. Metzner, and U. Schollwock, Phys. Rev. Lett. **86**, 4612 (2001).

[7] V. M. Loktev, R. M. Quick, and S. G. Sharapov, Phys. Rep. **349**, 1 (2001).

[8] Q. Chen, J. Stajic, S. Tan, and K. Levin, Phys. Rep. **412**, 1 (2005).

[9] A. Toschi, P. Barone, M. Capone, and C. Castellani, New J. Phys. **7**, 7 (2005).

[10] A. Garg, H. R. Krishnamurthy, and M. Randeria, Phys. Rev. B **72**, 024517 (2005).

[11] E. Zhao and A. Paramekanti, Phys. Rev. Lett. **97**, 230404 (2006).

[12] N. Dupuis, Phys. Rev. B **70**, 134502 (2004).

[13] M. Randeria, N. Trivedi, A. Moreo, and R. T. Scalettar, Phys. Rev. Lett. **69**, 2001 (1992).

[14] J. M. Singer, M. H. Pedersen, T. Schneider, H. Beck, and H.-G. Matuttis, Phys. Rev. B **54**, 1286 (1996).

[15] B. Kyung, A. Georges, and A.-M. S. Tremblay, Phys. Rev. B **74**, 024501 (2006).

[16] R. Blankenbecler, D. J. Scalapino, and R. L. Sugar, Phys. Rev. D **24**, 2278 (1981).

[17] E. Y. Loh, Jr. and J. E. Gubernatis, in *Electronic Phase Transitions*, edited by W. Hanke and Y. V. Kopaev (Elsevier, New York, 1992).

[18] S. R. White, D. J. Scalapino, R. L. Sugar, N. E. Bickers, and R. T. Scalettar, Phys. Rev. B **39**, 839 (1989).

[19] G. Grynberg, B. Lounis, P. Verkerk, J.-Y. Courtois, and C. Salomon, Phys. Rev. Lett. **70**, 2249 (1993).

[20] B. Uchoa and A. H. Castro Neto, Phys. Rev. Lett. **98**, 146801 (2007).

[21] B. Uchoa, G. G. Cabrera, and A. H. Castro Neto, Phys. Rev. B **71**, 184509 (2005).

[22] N. B. Kopnin and E. B. Sonin, Phys. Rev. Lett. **100**, 246808 (2008).

[23] B. Uchoa and A. H. Castro Neto, Phys. Rev. Lett. **102**, 109701 (2009).

[24] D. L. Bergman and K. Le Hur, Phys. Rev. B **79**, 184520 (2009).